Cation−Ether Complexes in the Gas Phase: Bond Dissociation Energies of M^+(dimethyl ether)$_x$, $x = 1-3$, M^+(1,2-dimethoxyethane)$_x$, $x = 1$ and 2, and M^+(12-crown-4) Where M = Rb and Cs

Michelle B. More,[†] Douglas Ray,*[,‡] and P. B. Armentrout*[,†]

Department of Chemistry, University of Utah, Salt Lake City, Utah 84112, and Environmental Molecular Sciences Laboratory, Pacific Northwest National Laboratory, Richland, Washington 99352

Received: May 16, 1997[⊗]

Bond dissociation energies of $M^+[O(CH_3)_2]_x$, $x = 1-3$; $M^+[(CH_2OCH_3)_2]_x$, $x = 1$ and 2; and $M^+[c\text{-}(C_2H_4O)_4]$, where M = Rb and Cs are reported. The bond dissociation energies (BDEs) are determined experimentally by analysis of the thresholds for collision-induced dissociation of the cation-ether complexes by xenon (measured using guided ion beam mass spectrometry). In all cases, the primary dissociation channel observed experimentally is endothermic loss of one ligand molecule. The cross section thresholds are interpreted to yield 0 and 298 K BDEs after accounting for the effects of multiple ion−molecule collisions, internal energy of the complexes, and unimolecular decay rates. The experimentally determined BDEs for the monodentate ligand complexes are in good agreement with conventional ideas of electrostatic ligation of gas-phase ions and with recent *ab initio* calculations by Feller et al. (average discrepancy of 5 ± 6 kJ/mol). The experimentally determined BDEs for the multidentate ligand complexes do not agree well with conventional ideas of electrostatic ligation of gas-phase ions or with recent *ab initio* calculations by Feller et al. (average discrepancy of 15 ± 5 kJ/mol per metal oxygen interaction). The presence of multiple conformers of the multidentate ligand complexes in the experimental apparatus is the likely cause of these large discrepancies.

Introduction

Many experimental and theoretical investigations have been undertaken to understand better the fundamental interaction between ions and neutral molecules and their relationship to molecular recognition.[1,2] These so-called "guest" and "host" molecules have excited many chemists with the prospect of designing host complexes that are highly selective for a particular guest ion. One host/guest system that has received much attention is the interaction of alkali metal cations with crown ethers. Crown ethers have been proposed for use in new chemical separations technologies[3] and in the development of advanced analytical methods.[4] Computational models capable of reliably predicting ligand selectivity in a variety of condensed-phase environments would be valuable tools for the advancement of this work. Such methods are currently under development; however, progress is hindered by a lack of suitable experimental data. One goal of the present work is to provide accurate experimental data to address this deficiency.

Over the past several years, there have been several qualitative[5−10] and semiquantitative[11] experimental investigations of alkali cation−crown ether complexes in the gas phase. Ion cyclotron resonance and tandem mass spectrometry have been employed to study these systems to obtain selectivities[7,9] via the kinetic method,[12] rates of complexation[6,8] bracketing reactions[7] and semi-quantitative bond dissociation energy (BDE) measurements.[11] Results of these studies are somewhat dependent upon the method of species generation (e.g., fast atom bombardment versus ion−molecule reactions) and the method of study (e.g., kinetic method versus bracketing reactions). These studies have motivated us to determine systematically the BDEs of the alkali ions bound to 12-crown-4 (12c4). Using kinetic energy-dependent collision-induced dissociation (CID), we have previously measured the binding energies of Li^+,[13,14] Na^+,[15] and K^+ [16] bound to one through four dimethyl ethers (DME), one and two 1,2-dimethoxyethanes (DXE), and 12c4. The smaller ligands were studied because the interpretation of the CID data for the monodentate DME ligands is much more straightforward compared to that for the bidentate DXE and tetradentate 12c4 ligands and to ascertain trends in the bonding as the complexity of the ligands was altered. Thus, the complete set of experiments helps ensure that reasonable thermochemistry is obtained. The present work is a continuation of these earlier studies and completes the series by providing results for Rb^+ and Cs^+ bound to the aforementioned set of ligands.

Experimental Section

General. Complete descriptions of the apparatus and the experimental procedures are given elsewhere.[17−19] The production of $M^+(L)_x$ (L = DME, DXE, and 12c4) complexes is described below. Briefly, ions are extracted from the source, accelerated, and focused into a magnetic sector momentum analyzer for mass analysis. Mass selected ions are retarded to a desired kinetic energy and focused into an octopole ion guide that radially traps the ions. The octopole passes through a static gas cell containing xenon, used as the collision gas for reasons described elsewhere.[20,21] After exiting the gas cell, product and undissociated reactant ions drift to the end of the octopole where they are focused into a quadrupole mass filter for mass analysis and subsequently detected by a secondary electron scintillation ion counter using standard pulse counting techniques. Raw ion intensities are converted to absolute cross sections as described previously.[18] Absolute uncertainties in cross section magnitudes are estimated to be ±20%, and relative uncertainties are ±5%.

Ion kinetic energies in the laboratory frame are related to center-of-mass (CM) frame energies by $E(\text{CM}) = E(\text{lab})\, m/(M + m)$, where M and m are the ion and neutral reactant masses, respectively. All energies cited below are in the CM frame

* Authors to whom correspondence should be addressed.
† University of Utah.
‡ Pacific Northwest National Laboratory.
⊗ Abstract published in *Advance ACS Abstracts,* August 15, 1997.

S1089-5639(97)01642-3 CCC: $14.00

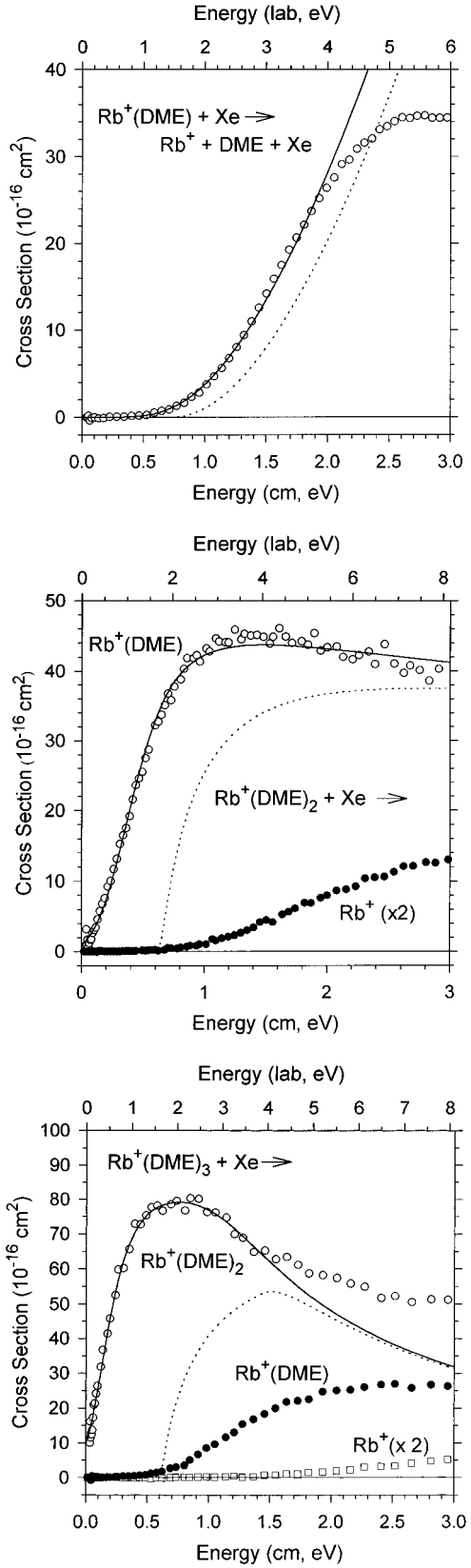

Figure 1. Cross sections for reactions of $Rb^+(DME)_x$, $x = 1-3$, with xenon (parts a−c, respectively) as a function of kinetic energy in the center-of-mass frame (lower x axis) and the laboratory frame (upper x axis). Open circles, filled circles, and open squares show cross sections for the primary, secondary, and tertiary products, respectively. The best fits to the data using the model of eq 3 incorporating RRKM modeling for the reactants with an internal temperature of 0 K are shown as dotted lines. Solid lines show these models convoluted over the kinetic and internal energy distributions of the reactant neutral and ion.

unless otherwise noted. Sharp features in the observed cross sections are broadened by the thermal motion of the neutral gas[22] and the distribution of ion energies. The zero of the absolute energy scale and the full width at half-maximum (fwhm) of the ion energy distribution are measured by a retarding potential technique described elsewhere.[18] The fwhm of the ion beam energy distribution was typically between 0.4 and 0.8 eV (lab) for these experiments. The uncertainty in the absolute energy scale is ±0.05 eV (lab).

The complexes are formed in a 1 m long flow tube[19] operated at a pressure of 0.4−0.7 Torr with a helium flow rate of 5000−7000 standard cm^3/min. Alkali metal ions are generated in a continuous dc discharge by argon ion sputtering of a cathode consisting of a carbon steel "boat" containing RbCl or CsCl salt. Complexes are formed by three-body associative reactions with the desired ligand introduced to the flow 5 cm downstream from the dc discharge. Typical operating conditions of the discharge are 3 kV and 30 mA in a flow of ∼4% argon in helium. The flow conditions used in this source provide approximately 10^5 collisions between the ions and the buffer gas, which should thermalize the complexes both rotationally and vibrationally to 300 K, the temperature of the flow tube. Previous work[23−27] has shown that this assumption is reasonable, and no evidence for nonthermal ions was observed in this work.

Experimental Results

$M^+(DME)_x$, $x = 1-3$. Experimental cross sections for the collision-induced dissociation (CID) of the $Rb^+(DME)_x$, $x = 1-3$, ion−molecule complexes with xenon are shown in Figure 1. Results for the $Cs^+(DME)_x$ complexes have a similar appearance and are shown in Figure 2. The sequential loss of intact DME molecules and ligand exchange with xenon to form $M^+(Xe)$ are the only processes observed in these systems over the 0−5 eV collision energy range studied. The cross sections for ligand exchange were small and thus data for these channels were not collected. The primary (both the lowest energy and dominant) process for all complexes is the loss of a single DME ligand in reaction 1.

$$M^+(DME)_x + Xe \rightarrow M^+(DME)_{x-1} + DME + Xe \quad (1)$$

As x increases, the primary cross section begins to decline more rapidly at higher energies because pathways for the primary product to decompose further by loss of additional DME ligands become more efficient. All complexes dissociate completely to the bare metal cation at high energies.

$M^+(DXE)_x$, $x = 1$ and 2. Experimental cross sections for the CID of the $Rb^+(DXE)_x$, $x = 1$ and 2, ion−molecule complexes with xenon are shown in Figure 3. Results for the $Cs^+(DXE)_x$ complexes have a similar appearance and are shown in Figure 4. The cross sections for ligand exchange are small, and thus data for these channels were not collected. The lowest energy and dominant process for all complexes is the loss of a single DXE ligand in reaction 2.

$$M^+(DX)_x + Xe \rightarrow M^+(DXE)_{x-1} + DXE + Xe \quad (2)$$

The $M^+(DXE)_2$ complexes in both metal systems lose both DXE ligands at elevated energies.

M^+(12c4). The experimental cross sections for the CID of Rb^+(12c4) with xenon and argon are shown in Figure 5. The experiment with Ar was performed to check for systematic errors in the results. The CID study with argon was performed on a different guided ion beam mass spectrometer than all other experiments reported here. It can be seen that even though the

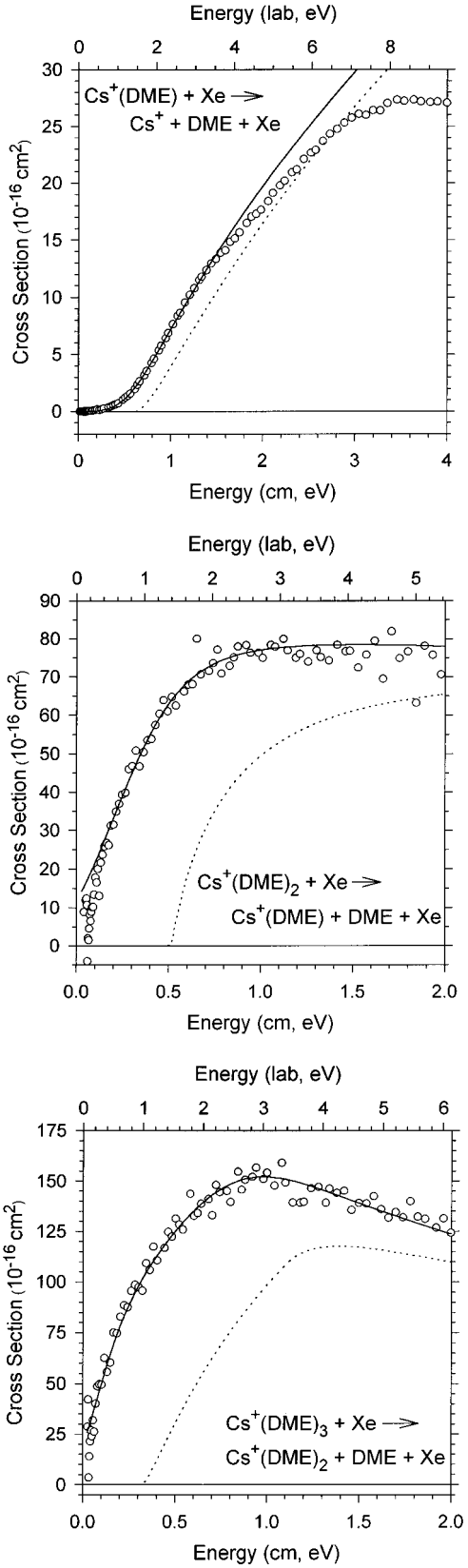

Figure 2. Cross sections for reactions of $Cs^+(DME)_x$, $x = 1-3$, with xenon (parts a−c, respectively) as a function of kinetic energy in the center-of-mass frame (lower x axis) and the laboratory frame (upper x axis). Open circles show cross sections for the primary products. The best fits to the data using the model of eq 3 incorporating RRKM modeling for the reactants with an internal temperature of 0 K are shown as dotted lines. Solid lines show these models convoluted over the kinetic and internal energy distributions of the reactant neutral and ion.

laboratory to center-of-mass energy conversion is quite different for the two collision gases, the results are equivalent. For both

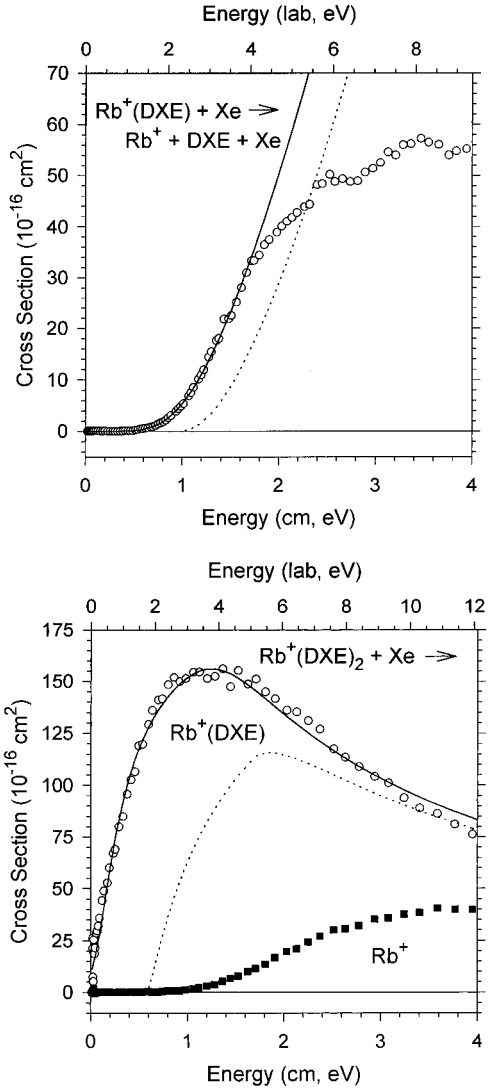

Figure 3. Cross sections for reactions of Rb+(DXE)x, $x = 1$ or 2, with xenon (parts a and b, respectively) as a function of kinetic energy in the center-of-mass frame (lower x axis) and the laboratory frame (upper x axis). Open circles and filled squares show cross sections for the primary and secondary products, respectively. The best fits to the data using the model of eq 3 incorporating RRKM modeling for the reactants with an internal temperature of 0 K are shown as dotted lines. Solid lines show these models convoluted over the kinetic and internal energy distributions of the reactant neutral and ion.

collision gases, no products other than Rb^+ and ligand exchange to form $Rb^+(Xe)$ are observed. Results for the CID of Cs^+-(12c4) with xenon have a similar appearance and are shown in Figure 6.

Thermochemical Analysis. Cross sections are modeled in the threshold region with eq 3,

$$\sigma = \sigma_0 \sum g_i (E + E_i + E_{rot} - E_0)^n / E \qquad (3)$$

where σ_0 is an energy-independent scaling factor, E is the relative translational energy of the reactants, E_0 is the threshold for reaction of the ground rotational, vibrational, and electronic state, E_{rot} is the rotational energy of the reactants, and n is an adjustable parameter. The summation is over i, which denotes the vibrational states of the complex, g_i is the population of those states ($\sum g_i = 1$), and E_i is the excitation energy of each vibrational state. Because the complexes studied here have many low-frequency vibrational modes, the populations of excited vibrational levels are not negligible at 298 K. The Beyer−Swinehart algorithm[28] is used to calculate the population

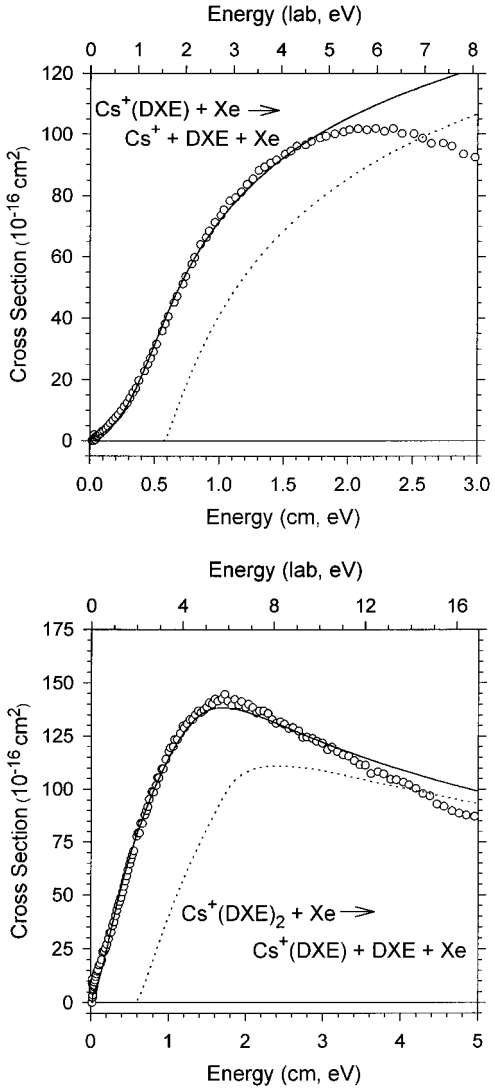

Figure 4. Cross sections for reactions of $Cs^+(DXE)_x$, $x = 1$ and 2, with xenon (parts a and b, respectively) as a function of kinetic energy in the center-of-mass frame (lower x axis) and the laboratory frame (upper x axis). Open circles show cross sections for the primary produccts. The best fits to the data using the model of eq 3 incorporating RRKM modeling for the reactants with an internal temperature of 0 K are shown as dotted lines. Solid lines show these models convoluted over the kinetic and internal energy distributions of the reactant neutral and ion.

of the vibrational levels using the frequencies listed in Table 1. Frequencies for free DME have been taken from Shimanouchi.[29] Scaled (85, 90, and 100%) vibrational frequencies for free 1,2-dimethoxyethane, free 12c4, and all rubidium and cesium cation complexes are taken from theoretical calculations of Feller and co-workers.[30,31] For several of the multiligated complexes, the vibrations having the lowest frequencies had calculated values that were imaginary due to the finite difference method used. As a first approximation, imaginary frequencies were simply set equal to 3 or 1 cm^{-1} depending on the frequencies calculated for the analogous complexes with K^+. These revised frequencies are underlined in Table 1. An alternate, and probably more reliable, approach used in some of the analyses was to assign these frequencies as rotors, consistent with the nuclear motion that they describe.

The form of eq 3 is expected to be appropriate for translationally driven reactions[32] and has been found to reproduce cross sections well in a number of previous studies of both atom−diatom and polyatomic reactions,[33,34] including CID processes. In our analysis of $M^+(DME)_x$, $x = 3$, we also use a modified

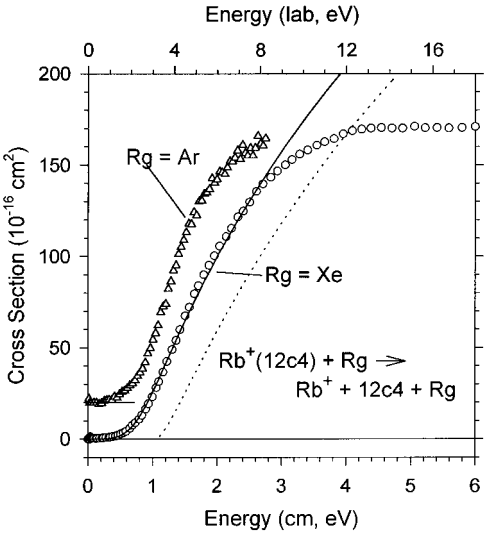

Figure 5. Cross sections for the reaction of $Rb^+(12c4)$ with xenon and argon as a function of kinetic energy in the center-of-mass frame (lower x axis) and the laboratory frame (upper x axis). Open circles and open triangles show cross sections for the primary product ion produced from CID with xenon and argon, respectively. The argon data has been offset for clarity. The best fit to the xenon data using the model of eq 3 incorporating RRKM modeling for the reactants with an internal temperature of 0 K is shown as a dotted line. The solid line shows this model convoluted over the kinetic and internal energy distributions of the reactant neutral and ion.

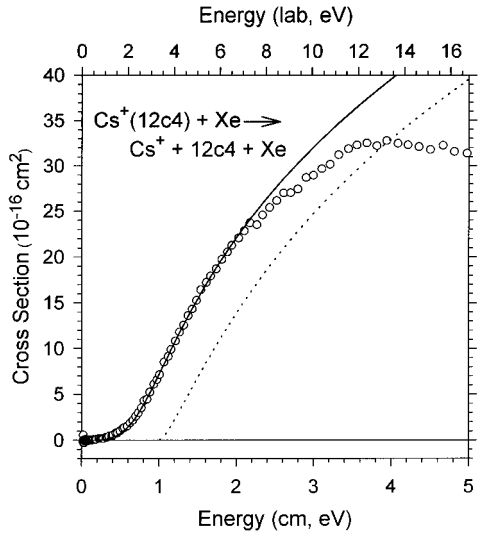

Figure 6. Cross sections for the reaction of $Cs^+(12c4)$ with xenon as a function of kinetic energy in the center-of-mass frame (lower x axis) and the laboratory frame (upper x axis). Open circles show the cross section for the primary product ion. The best fit to the data using the model of eq 3 incorporating RRKM modeling for the reactants with an internal temperature of 0 K is shown as a dotted line. The solid line show this model convoluted over the kinetic and internal energy distributions of the reactant neutral and ion.

form of eq 3 that accounts for a decline in the product ion cross section at higher kinetic energies. This model has been described in detail previously[36] and depends on E_D, the energy at which a dissociation channel begins, and p, a parameter similar to n in eq 3.

Because the rotational, vibrational, and translational energy distributions are explicitly included in our modeling, the threshold energies determined using eq 3 correspond to 0 K. The threshold energies determined for CID reactions are converted into 0 K BDEs by assuming that E_0 represents the energy difference between the reactants and the products at 0 K.[37] This requires that there are no activation barriers in excess

TABLE 1: Vibrational Frequencies and Average Vibrational Energies at 298 K[a] for Rb^+ and Cs^+ Complexes and Ligands

species	E_{vib}[a] eV	frequencies[b] (degeneracies), cm^{-1}
DME	0.04	203, 242, 418, 928, 1102, 1150, 1179, 1227, 1244, 1452(2), 1464(4), 2817(2), 2925, 2952, 2996(2)
DXE	0.14(0.01)	68, 110, 118, 144, 209, 229, 319, 383, 487, 814, 955, 1006, 1055, 1140, 1155, 1164, 1167, 1180, 1224, 1232, 1238, 1286, 1357, 1444, 1467, 1478, 1481(2), 1490, 1491, 1509, 1516, 2862, 2863, 2875, 2876, 2893, 2911, 2918(2), 2984, 2985
12c4	0.27(0.02)	60, 82, 126(2), 146(2), 232, 241(2), 297, 346, 353(2), 363, 460, 517(2), 558, 778, 814(2), 858, 898, 912(2), 933, 1017, 1039(2), 1045, 1094, 1120(2), 1140, 1173, 1176(2), 1184, 1256, 1264(2), 1270, 1286, 1308(2), 1326, 1372, 1391(2), 1409, 1425, 1435(2), 1438, 1482(2), 1483, 1484, 1494(3), 1500, 2857(3), 2858, 2892, 2894(2), 2897, 2935, 2936(2), 2937, 2959, 2960(2), 2963
Rb^+(DME)	0.10(0.01)	**71**, **87**, 111, 173, 245, 406, 905, **1085**, 1148, 1177, 1182, 1263, 1452, 1468, 1481, 1485, 1489, 1495, 2894, 2901, 2965(2), 2977, 2980
Rb^+(DME)$_2$	0.29(0.01)	**3**, **4**, **5**, **68**(**2**), 82, 84, 95, 113, 176(2), **244**(2), 404, 405, 906, 909, 1087, 1088, 1148(2), 1180, 1181, 1183(2), 1263(2), 1452(2), 1469, 1470, 1481(2), 1485(2), 1488(2), 1496(2), 2891(2), 2898(2), 2958(2), 2959(2), 2977(2), 2979(2)
Rb^+(DME)$_3$	0.47(0.02)	**3**, **5**, **6**, **7**(**2**), 13, 64, 66(2), 78, 79, 81, 82, 106(2), 178(2), 179, 243(3), **403**(2), 404, 909(2), 914, 1090, 1091(2), 1148(2), 1149, 1183(4), 1184(2), 1263(3), 1452(3), 1470(2), 1471, 1481, 1482(2), 1485(3), 1487(3), 1496(2), 1497, 2887(3), 2895(3), 2953(5), 2954, 2976(3), 2978(2), 2979
Rb^+(DXE)	0.20(0.01)	35, 87, 96, 106, 113, 137, **192**, **210**, 288, 329, 342, **543**, 839, 852, 1013, 1034, 1104, 1108, 1139, 1163, 1168, 1213, 1227, 1261, 1306, 1400, 1440, 1470, 1475, 1477(2), 1488(2), 1499, 1501, 2887, 2891, 2895, 2898, 2928, 2939, 2957(2), 2983(2)
Rb^+(DXE)$_2$	0.48(0.02)	**1**(**2**), **2**, 36, 37, **67**, 79(2), 96, 100(2), 101, 118, 132, 133, **198**(**2**), 212(2), 286(2), 323(2), 340(2), 545(2), 843(2), 852, 854, 1015, 1017, 1038(2), 1108(2), 1112(2), 1145(2), 1165(2), 1169(2), 1216(2), 1228(2), 1262(2), 1305(2), 1400(2), 1441(2), 1470(2), 1474(2), 1477(2), 1478(2), 1488(2), 1489(2), 1499(2), 1501(2), 2881(2), 2885(2), 2890(2), 2893(2), 2921(2), 2931(2), 2949, 2950(3), 2982(4)
Rb^+(12c4)	0.31(0.02)	58, **86**(2), 104, 106, **132**, **191**(2), 193, 245, 258(2), 280, 329, 347(2), 397, 477, 535(2), 579, 788, 804(2), 844, 887, 905, 907(2), 1029, 1035(2), 1050, 1069, 1113(2), 1136, 1158, 1163(2), 1172, 1254, 1264(2), 1276, 1280, 1304(2), 1318, 1370, 1390(2), 1406, 1429, 1433(2), 1434, 1484(3), 1485, 1493, 1501(2), 1514, 2889, 2894(2), 2895, 2907, 2911(2), 2916, 2924, 2931(2), 2941, 2964, 2966(2), 2968
Cs^+(DME)	0.11(0.01)	**66**, **83**, 91, 175, 244, 404, 907, **1088**, 1148, 1180, 1182, 1262, 1452, 1467, 1481, 1485, 1488, 1496, 2891, 2898, 2959(2), 2975, 2978
Cs^+(DME)$_2$	0.29(0.01)	**3**, **5**, **8**, **64**, **65**, 79, 81, 84, 89, 179(2), **243**(2), 403(2), 908, 912, 1091(2), 1148(2), 1183(3), 1184, 1263(2), 1452(2), 1470, 1471, 1481, 1482, 1486(2), 1488(2), 1496, 1497, 2887(2), 2895(2), 2953(2), 2954(2), 2975(2), 2977(2)
Cs^+(DME)$_3$	0.48(0.02)	**3**(**3**), **5**(**2**), 9, 60, 62(2), 71, 75, 76, 77, 85, **86**, 180(3), 242(3), 402(2), 403, 911(2), 914, 1093(3), 1149(3), 1183(3), 1185, 1186(2), 1263(3), 1452(3), 1471(3), 1482(3), 1486(3), 1487(3), 1497(3), 2885(3), 2894(3), 2949(6), 2975(3), 2977(2), 2978
Cs^+(DXE)	0.20(0.01)	33, 76, 85, 100, 103, 131, 194, 211, 288, 326, 340, 543, 842, 851, 1015, 1036, 1107, 1110, 1142, 1164, 1168, 1215, 1227, 1261, 1307, 1400, 1441, 1470, 1475, 1477, 1478, 1488, 1490, 1499, 1501, 2883, 2887, 2893, 2895, 2923, 2934, 2951, 2952, 2979, 2980
Cs^+(DXE)$_2$	0.49(0.02)	**1**(**3**), 4(2), **61**, 68(2), 87, 95(2), 99(2), 130, 131, **199**(**2**), 212(2), 285(2), 320(2), 339(2), 545(2), 845(2), 851, 853, 1017, 1019, 1039(2), 1107(2), 1116(2), 1148(2), 1165(2), 1169(2), 1217(2), 1228(2), 1262, 1265, 1306(2), 1400(2), 1441(2), 1470(2), 1474(2), 1478(3), 1479, 1488(2), 1489(2), 1499(2), 1501(2), 2878(2), 2882(2), 2887(2), 2891(2), 2918(2), 2929(2), 2945, 2946(3), 2978(2), 2979(2)
Cs^+(12c4)	0.31(0.02)	56, **72**(2), 84, 102, **131**, **190**, 191(2), 245, 256(2), 279, 329, 347(2), 397, 476, 535(2), 579, 788, 805(2), 843, 887, 905, 907(2), 1030, 1036(2), 1050, 1070, 1114(2), 1139, 1161, 1165(2), 1173, 1255, 1265(2), 1277, 1282, 1305(2), 1319, 1370, 1391(2), 1407, 1429, 1433(2), 1436, 1484(3), 1485, 1493, 1501(2), 1514, 2887, 2891(2), 2892, 2903, 2908(2), 2912, 2921, 2930(2), 2940, 2962, 2963(2), 2966

[a] Uncertainties, listed in parentheses, are determined as one standard deviation of the RHF frequencies scaled by 1.0, 0.9, and 0.85. [b] All vibrational frequencies except for those of DME are RHF frequencies taken from refs 30 and 31 scaled by 0.9. Experimental DME freqencies are taken from ref 29. Transitional mode frequencies are in boldface with the reaction coordinate being the largest of these values. All underlined vibrational frequencies were originally imaginary RHF calculated values. The imaginary values were changed into real values that are similar to those in the analogous complexes with K^+.[16]

of the endothermicity. This is generally true for ion−molecule reactions[33,38] and should be valid for the simple bond fission reactions studied here.[39] This conclusion needs more careful consideration in the case of the multidentate DXE and 12c4 ligands where the conformation of the ligand changes in going from the lowest energy state of the complex to the lowest energy form of the products. For the DXE and 12c4 ligands, barriers separating these conformations in the absence of the metal ion are likely to be small. We believe that the energy of complexation with the metal ion can overcome any such barriers to rearrangement. In essence, dissociation of the lowest energy conformation of the complex to the products should have no barriers in excess of the bond energy as long as the interaction between the metal cation and the ligand in its lowest energy conformation is attractive at long range. This presumes that barriers between conformations of the complex are less than the binding energy of the metal ion to the ligand; exceptions seem unlikely. Thus, the question of conformations moves from an energetic one to a kinetic one, namely, in the presence of multiple conformations, what is the rate at which the excited complex moves along the lowest energy dissociation path. Given the flexibility of the empirical model used to determine the threshold for dissociation, it seems likely that the true thresholds are still accurately located even if the unimolecular rate constant does not include such an effect explicitly. In the end, comparison of the thermochemistry measured here to theoretical work provides some test of this conclusion. This is discussed below.

Other considerations in the analysis of CID thresholds are the presence of nonthermalized ions, pressure effects, and the lifetime of the complex after collisional excitation. These considerations are treated as follows. First, excess internal excitation is unlikely because the ions that traverse the 1 m flow tube undergo 10^5 collisions with the buffer gases. Second, pressure effects due to multiple collisions with Xe are examined by performing the experiments at three different pressures.

Pressure effects are eliminated, following a procedure developed previously,[40] by linearly extrapolating the cross sections to zero-pressure, rigorously single-collision conditions. It is these cross sections that are further analyzed. Pressure effects were present for the Rb + $(DME)_x$ complexes, Rb^+ and Cs^+ singly ligated DXE complexes, $Cs^+(DXE)_2$, and the Rb^+ and Cs^+ 12c4 complexes. The pressure effects are most critical at low energies where the threshold cross sections begin to rise. In the case of Rb^+(12c4), cross sections of even low-pressure data (0.040 mTorr) were shifted down in energy by as much as 0.05 eV (compared to data extrapolated to zero pressure) at collision energies less than 1 eV.

The lifetime effect is examined by incorporating RRKM theory into eq 3 as previously detailed[25,41] employing the *phase space limit* transition state, *PSL* TS, model and a *loose* TS model.[15] The additional information necessary to implement this theory is the set of vibrational frequencies for the transition state (TS) associated with the dissociation. This choice is reasonably straightforward because the TS should be fairly loose and similar to the CID products. Thus, most of the frequencies for both the *PSL* and *loose* TS models are those of the products, $M^+(L)_{x-1}$ + L, which are listed in Table 1.

The difference between the *PSL* and *loose* TS models is how they treat the transitional modes, usually hindered rotations, bends, and torsions, of the energized molecule. For both models, the transitional mode frequencies (those affected most severely as the ligand is removed) are in boldface in Table 1 and chosen as follows. One M^+−L stretching frequency is chosen as the reaction coordinate and removed. For the *loose* TS model, the five [two for M^+(DME), M^+(DXE), and M^+-(12c4)] remaining frequencies of the M^+(L) reactant are modified by dividing these frequencies by 2 and 10 to give a range in the looseness of the TS. The E_0s obtained with these modified TS parameters are averaged to yield E_0*(loose)*. For the *PSL* TS model, the transitional modes are assigned as free rotors of the products as described elsewhere.[41−43] We also determine a threshold energy for a tight TS, E_0*(tight)*, and a threshold energy without RRKM lifetime modeling to quantify the kinetic shift. The tight TS is obtained by removing only the reaction coordinate frequency and leaving the other frequencies unchanged.

All of the TSs are characterized by an entropy of activation, $\Delta S^\dagger$, the difference in entropy between the energized molecule and the transition state. These are calculated using the vibrational frequencies given in Table 1 and rotational constants calculated by Feller and co-workers.[30,31] For some of the complexes studied here, it is possible that there is a distribution of energetically similar conformations such that the entropies are not accurate. Unfortunately, a calculation that properly treats such a distribution cannot be performed without molecular parameters for each conformation and accurate relative energy information, neither of which are available. Failure to account for such a possibility is not a major concern because the primary purpose of the $\Delta S^\dagger$ calculation is as a measure of the *relative* looseness of the transition state for dissociation, which is not affected by the multiple conformations of the complex.

Many of the calculated entropies of activation, $\Delta S^\dagger$, for the *PSL* model are negative, which indicates a relatively tight transition state in contrast to the desired character of the *PSL* TS. The reason for these negative entropies lies with the unreasonably low vibrational frequencies of the energized molecule (those <10 cm^{-1}) for many of the complexes. Because these low vibrational frequencies correspond to very floppy motions, they are difficult to calculate accurately. Because these frequencies are unreasonably low, the number of accessible states for the energized molecule at 1000 K is overcounted and its entropy overestimated. In the loose TS model, reasonable entropies of activation are found because the transitional modes were obtained by dividing the very low frequencies of the energized molecule by factors of 2−10. Although this retains absurdly low vibrational frequencies, the treatment is self-consistent since the number of accessible state for the TS at 1000 K are also over counted. In contrast, the *PSL* model for the activated complex replaces these very low frequencies with the corresponding free rotors of the incipient products. This leads to a more accurate counting of the accessible states at 1000 K for the activated complex, but a procedure that is inconsistent with that for the energized molecule. To correct for this overcounting, we also analyzed the data with a modified version of the *PSL* TS model, which we will refer to as *PSLR*, in which the low vibrational frequencies of the energized molecules were assigned as free rotors instead. Rather than replace only those frequencies that we arbitrarily decided were too low, we replaced vibrations with rotations in both the energized molecule and activated complex using the following procedure. For species with one ligand, M^+(L), the two lowest vibrational frequencies were replaced with the 2D rotational constant of the ligand. (The 1D rotational constant already describes the overall 1D rotation of the complex.) For species with two ligands, $M^+(L)_2$, the six lowest vibrational frequencies were replaced with two sets of rotational constants (a 1D and a 2D rotor per set) for the associated ligand. For species with three ligands, $M^+(L)_3$, the nine lowest vibrational frequencies were replaced with three sets of rotational constants for the associated ligand.

Before comparison with experimental data, the model of eq 3 was convoluted with the kinetic energy distributions of the reactants.[18] The parameters σ_0, n, and E_0 were then optimized with a nonlinear least-squares analysis to give the best fit to the data. An estimate of the error in the threshold energy is obtained from variations in E_0 for different data sets, variations in the parameter n, variations associated with uncertainties in the vibrational frequencies, and the error in the absolute energy scale. Uncertainties listed with the E_0 (*PSLR*), E_0 *(PSL)*, E_0 *(loose)*, and E_0*(tight)* values also include errors associated with variations in the time assumed for dissociation (10^{-4} s) by factors of 2 and 0.5. Uncertainties for the E_0 *(loose)* and associated $\Delta S^\dagger$ values include variations in the transitional frequencies as mentioned above.

Results for the analysis of the cross sections shown in Figures 1−3 with eq 3 are provided in Table 2. These thresholds are equivalent to BDEs at 0 K. As established in previous work,[15,16,41,43] the *tight* TS values can be viewed as very conservative lower limits to the correct thermodynamics, while values obtained with no RRKM modeling provide very conservative upper limits. Generally, we have found that the *PSL* TS values provide the most accurate thermochemistry with *loose* TS values being very similar. In the present system, the *PSL* and *loose* TS values are again similar and also similar to the values obtained by the alternate *PSLR* TS treatment. Because the very low vibrational frequencies make the accuracy of the *PSL* treatment suspect for the present systems, we conservatively assign our best values as an average of the thresholds obtained with the *PSL*, *loose*, and *PSLR* treatments. These average values are presented in Table 3 after conversion to 298 K values. The conversion of BDEs from 0 to 298 K is achieved using standard formulas for the temperature dependence of the enthalpy.[44] The temperature correction for the BDEs of Rb^+ and Cs^+ complexes is given as $\Delta\Delta H$ in Table 3.

TABLE 2: Bond Dissociation Energies at 0 K and Entropies of Activation at 1000 K for $M^+(DME)_x$, $x = 1-3$, $M^+(DXE)_x$, $x = 1$ and 2, and $M^+(12c4)$ Where M = Rb and Cs[a]

species	E_0,[b] eV	E_0(*PSLR*), eV	$\Delta S^\dagger_{1000}$ (*PSLR*), J/(mol K)	E_0(*PSL*), eV	$\Delta S^\dagger_{1000}$ (*PSL*), J/(mol K)
Rb^+(DME)	0.69(0.12)	0.62(0.09)	56	0.60(0.09)	29
$Rb^+(DME)_2$	0.59(0.04)	0.56(0.04)	19	0.58(0.04)	−17
$Rb^+(DME)_3$	0.5(0.06)	0.41(0.09)	28	0.36(0.09)	−11
Rb^+(DXE)	1.10(0.03)	0.92(0.07)	23	0.98(0.07)	35
$Rb^+(DXE)_2$	0.75(0.05)	0.55(0.05)	35	0.53(0.05)	−29
Rb^+(12c4)	1.19(0.04)	0.86(0.07)	36	1.06(0.07)	68
Cs^+(DME)	0.61(0.03)	0.61(0.04)	1	0.57(0.04)	7
$Cs^+(DME)_2$	0.52(0.03)	0.50(0.05)	14	0.52(0.05)	−10
$Cs^+(DME)_3$	*c*	0.49(0.03)	42	0.36(0.03)	−28
Cs^+(DXE)	0.67(0.04)	0.59(0.03)	13	0.61(0.03)	31
$Cs^+(DXE)_2$	0.72(0.06)	0.61(0.04)	44	0.52(0.04)	−31
Cs^+(12c4)	1.03(0.08)	0.80(0.05)	24	0.96(0.05)	51

species	E_0(*loose*), eV	$\Delta S^\dagger_{1000}$ (*loose*), J/(mol K)	E_0(*tight*), eV	$\Delta S^\dagger_{1000}$ (*tight*), J/(mol K)
Rb^+(DME)	0.70(0.10)	34(19)	0.58(0.08)	9
$Rb^+(DME)_2$	0.57(0.05)	43(43)	0.50(0.02)	−4
$Rb^+(DME)_3$	0.36(0.11)	105(47)	0.20(0.07)	−11
Rb^+(DXE)	1.00(0.07)	10(19)	0.98(0.07)	12
$Rb^+(DXE)_2$	0.46(0.17)	63(47)	0.31(0.04)	−3
Rb^+(12c4)	0.95(0.11)	49(19)	0.87(0.11)	−3
Cs^+(DME)	0.59(0.03)	14(19)	0.57(0.04)	11
$Cs^+(DME)_2$	0.46(0.05)	69(47)	0.43(0.04)	0
$Cs^+(DME)_3$	0.39(0.090	101(47)	0.19(0.04)	−7
Cs^+(DXE)	0.58(0.06)	−17(19)	0.58(0.06)	−11
$Cs^+(DXE)_2$	0.55(0.07)	55(48)	0.41(0.04)	−5
Cs^+(12c4)	0.88(0.05)	33(20)	0.86(0.03)	9

[a] Uncertainties (one standard deviation) are listed in parentheses. [b] No RRKM lifetime analysis. [c] Data could not be modeled well without incorporating the RRKM lifetime effect into eq 1.

TABLE 3: Bond Dissociation Enthalpies at 298 K and Enthalpy Shifts of $M^+(DME)_x$, $x = 1-3$, $M^+(DXE)_x$, $x = 1$ and 2, and $M^+(12c4)$ Where M = Rb and Cs in kJ/mol[a]

species	ΔH_{298}(CID)	ΔH_{298}(MP2)[b]	$\Delta\Delta H$[c]
Rb^+−(DME)	64(9)	66	2.1
(DME)Rb^+−(DME)	51(5)	54	−3.7
$(DME)_2Rb^+$−(DME)	33(11)	49	−3.7
Rb^+−(DXE)	95(9)	110	0.6
(DXE)Rb^+−(DXE)	46(12)	83	−3.4
Rb^+−(12c4)	95(13)	164	2.2
Cs^+−(DME)	57(5)	57	0
(DME)Cs^+−(DME)	43(6)	46	−3.8
$(DME)_2Cs^+$−(DME)	36(9)	41	−3.9
Cs^+−(DXE)	57(5)	94	0
(DXE)Cs^+−(DXE)	50(7)	70	−3.6
Cs^+−(12c4)	86(9)	140	1

[a] Uncertainties (one standard deviation) are listed in parentheses. [b] 6-31+G* values taken from refs 30 and 31. [c] $\Delta\Delta H$ is the enthalpy shift of the ion complex from 298 to 0 K, $\Delta H_{298} - \Delta H_0$. The enthalpy corrections were determined using the vibrational frequencies listed in Table 1.

Discussion

Comparison of Experimental and Theoretical Bond Dissociation Energies. Table 3 compares our experimental values with the theoretical results of Glendening, Hill, and Feller[30,31] for the BDEs at 298 K of the DME, DXE, and 12c4 complexes with Rb^+ and Cs^+. In this theoretical work, equilibrium gas-phase geometries were optimized using a modified 6-31+G* basis set[45] at the second-order Møller−Plesset perturbation level of theory (MP2) for $M^+(DME)_x$, $x = 1$ and 2, and at the restricted Hartree−Fock (RHF) level of theory for $M^+(DME)_x$, $x = 3$ and 4, $M^+(DXE)_x$, $x = 1$ and 2, and $M^+(12c4)$.

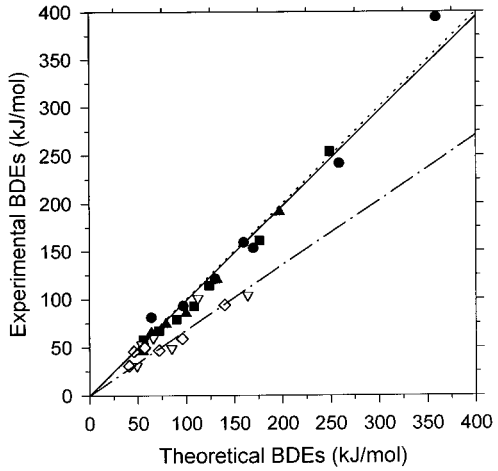

Figure 7. Experimental bond dissociation energies at 298 K in kJ/mol are plotted against the respective theoretical bond dissociation energies. Solid symbols refer to $M^+(DME)_x$, $x = 1-4$, $M^+(DXE)_x$, $x = 1$ and 2, and $M^+(12c4)$ for M = Li (circles), Na (square), and K (triangles) complexes. Open symbols refer to M = Rb (inverted triangles) and Cs (diamonds) complexes. The solid line is a linear regression (constrained to pass through the origin) of the M = Li, Na, and K points. The dash-dot line is a linear regression (constrained to pass through the origin) of the $M^+(DXE)_x$ and $M^+(12c4)$ data for M = Rb and Cs points. The dotted line has a slope of unity. Experimental BDEs are taken from refs 11−14 and the present work. Theoretical BDEs are taken from refs 13, 14, 30, and 31.

Correlation corrections were evaluated with frozen-core (the eight valence electrons are included in the correlation), MP2 theory applied to the optimized geometries. Undesirable basis set superposition errors in the calculated bond energies were estimated with the full counterpoise correction. The theoretical bond dissociation energies are fairly sensitive to the size and completeness of the basis set used, a point recently evaluated for potassium ion−ether complexes in some detail by Feller et al.[46] In that work, it is estimated that BDEs calculated at the MP2 level of theory with the 6-31+G* basis set and counterpoise corrected should be accurate to within ±13 kJ/mol of the complete basis set (CBS) limit.

Table 3 shows that the theoretical and experimental values are in reasonable agreement for the monodentate DME ligand complexes, with an average discrepancy of 5 ± 6 kJ/mol. Only the BDE for $Rb^+(DME)_3$ differs by more than the experimental error. For the DXE and 12c4 complexes, agreement is not as gratifying, with large discrepancies observed in most cases. For these multidentate ligands, the average difference is 15 ± 5 kJ/mol per metal oxygen interaction.

There are a number of possible explanations for these discrepancies. Previous work has shown that BDEs for alkali ion−ether complexes obtained by threshold CID and by *ab initio* calculations at this level agree well, presumably an indication of good accuracy of both the experiments and the calculations. This is shown in Figure 7, which compares experimental and theoretical bond energies for Li^+, Na^+, K^+, Rb^+, and Cs^+ with 1−4 DME ligands, 1 and 2 DXE ligands, and 12c4. For the three lighter alkali ions, the agreement is very good. A linear regression analysis (constrained to pass through the origin) of the points for the Li^+, Na^+, and K^+ complexes yields a slope of 0.99 ± 0.02. The BDEs for Rb^+ and Cs^+ bound to 1−3 to three DME ligands fall on the same line, with experimental BDEs that average 10 ± 12% lower than the theoretical BDEs. In contrast, the BDEs for Rb^+ and Cs^+ bound to DXE and 12c4 appear to form a distinct subset of values, with experimental values averaging 35 ± 11% lower than the theoretical values. Of course, it is possible that the theoretical calculations in these

large systems are less accurate because of the relatively small basis set size and the frozen-core approximation necessary to deal with the very heavy metal ions. However, these approximations do not appear to be problematic for the analogous K^+ complexes.[16] Further, if this were the main problem, it is unclear why the results for Rb^+ and Cs^+ complexes with DME would differ from those with DXE and 12c4.

Another possibility is that our experimental data analysis has overestimated the lifetime effect for these complexes. As noted above, the *PSL* and *loose* TS models have proven to provide fairly accurate information in a number of previous systems, but it is possible that the weaker bonds involved here could change the observed dynamics (although this should be less true for the more strongly bound multidentate ligands than for the monodentate ligands). One way of assessing this possibility is to examine threshold energies obtained assuming that dissociation always occurs more rapidly than the experimental time scale, i.e., the E_0 values with no RRKM analysis listed in Table 2. These experimental BDEs are larger than those cited in Table 3. For most of the DME complexes, these numbers still agree with theory, but the experimental values for $Rb^+(DME)_3$, Rb^+-(DXE), and $Cs^+(DXE)_2$ are now within experimental error of the theoretical values. These experimental values for Rb^+-$(DXE)_2$, Rb^+(12c4), Cs^+(DXE), and Cs^+(12c4) are still much lower than the theoretical values. As a consistent interpretation of the data is warranted, it does not appear that lifetime effects can adequately explain the discrepancies either.

Another possible explanation for these discrepancies is that the complexes are internally excited. This would lower the apparent threshold, making the experimentally derived BDEs too low. To test this hypothesis, we checked whether results for Rb^+(12c4) changed when this complex was generated on a different apparatus. Although these two guided ion beam tandem mass spectrometers are similar,[17,18] there are distinct differences in the flow conditions accessible and details of the differential pumping. We also changed the collision gas from Xe to Ar to examine whether there were any differences in dynamics and to provide more precision in the energy scale because of the larger laboratory to center-of-mass energy scale conversion factor. As shown in Figure 5, the results with Ar are basically identical to the data with Xe, indicating no obvious effects associated with incomplete cooling or collisional dynamics.

To ascertain whether the theoretical or experimental BDEs are most reasonable, we compare the trends in these values to those for the analogous K^+ complexes.[16] In previous work,[16] we have found that comparisons of the BDEs for Na^+ and K^+ complexes with these ethers are very well correlated with one another. Figure 8 shows the experimentally and theoretically[30,31] determined BDEs of the Rb^+ and Cs^+ complexes plotted against the BDEs of the analogous K^+ complexes. For both the Rb^+ and Cs^+ systems, the theoretical BDEs are well correlated with the BDEs of the K^+ complexes. Linear regression analysis of these data yield slopes of 0.84 and 0.72, respectively. Not surprisingly, this indicates that the complexes of K^+ are bound more strongly than the analogous complexes of Rb^+, which are stronger than those of Cs^+. This is simply because the smaller alkali ions have shorter bond lengths and thus stronger interactions. Experimental BDEs for Rb^+ and Cs^+ with the DME ligands are found to lie close to these lines, but there are substantial deviations for the experimental BDEs for the complexes of Rb^+ and Cs^+ with the multidentate ligands other than Rb^+(DXE). These comparisons suggest that the experimentally determined BDEs for the multidentate complexes are anomalously low.

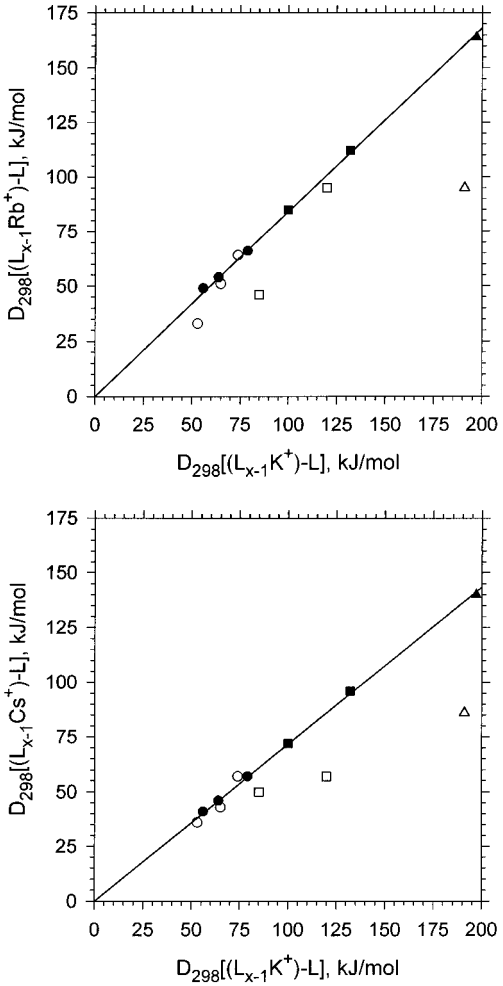

Figure 8. Experimental and theoretical bond dissociation enthalpies in kJ/mol at 298 K of $M^+(DME)_x$, $x = 1-3$, $M^+(DXE)_x$, $x = 1$ and 2, and M^+(12c4) for M = Rb and Cs (parts a and b, respectively) plotted against the BDEs for the analogous K^+ complexes. Open and solid symbols refer to experimental and theoretical values, respectively. Circle, squares, and triangles refer to the $M^+(DME)_x$, $M^+(DXE)_x$, and M^+(12c4) complexes, respectively. The solid line in each figure is a linear regression (constrained to pass through the origin) of the theoretical points. The experimental BDEs for the K+ complexes are taken from ref 16, and the theoretical BDEs are taken from refs 30 and 31.

Excited Conformers? One possible explanation for anomalously low experimental BDEs is that they do not correspond to the minimum-energy conformation of the complex; rather, we are measuring BDEs of excited conformations. For this scenario to be plausible, the excited conformation must be formed easily from the separated metal ion and ligands, while the formation of the minimum-energy conformer requires additional rearrrangement. In addition, there must be a barrier that prevents the excited conformations from rearranging to the minimum-energy conformation when the complexes are formed and thermalized. A potential energy surface corresponding to this scenario is illustrated in Figure 9. Of course, a mixture of both conformers could be formed in the experimental apparatus, however, the threshold measured would correspond to the higher energy (lower bond energy) species as long as there is an appreciable population of this conformer. This condition also makes it very difficult to observe a higher energy process that could correspond to the threshold for dissociation of a ground state species. No obvious indications of such processes are observed in the cross sections obtained here.

An excited conformer seems plausible for the M^+(12c4) complex. When uncomplexed, 12c4 has a minimum-energy

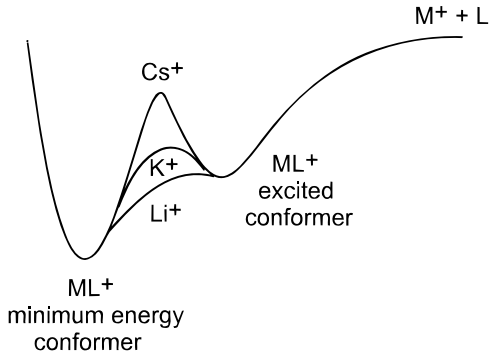

Figure 9. A potential energy diagram describing the formation of the alkali cation−ligand complexes, $M^+(L)$, in the minimum-energy and a low-lying excited conformation starting from the separated alkali cation, M^+, and ligand, L.

geometry with S_4 symmetry that is quite different from the C_4 geometry of the ligand when it is complexed (see Figures 3 and 4 of ref[21]). A critical difference in these two geometries is the orientation of the oxygen atoms in the ring. The S_4 geometry has two oxygens pointing to one side of the ring and two pointing to the other side, such that the oxygen dipoles interact weakly with one another. In the C_4 geometry, all of the oxygen atoms point to one side of the ring, such that an alkali cation can interact strongly with all four oxygen atoms. In generating the alkali ion-crown complexes in a flow tube source, the metal ion interacts with the S_4 geometry crown and is then stabilized by three-body collisions. The question is whether the two oxygen atoms pointing away from the alkali ion can overcome the barrier necessary to turn through the middle of the ring and toward the alkali ion. It seems reasonable that if the alkali ion is small, the electrostatic field pulling the oxygens toward the ion could be sufficiently strong that this rearrangement barrier can be overcome. Thus, no problems with forming the ground state of the M^+(12c4) complexes for M = Li, Na, and K were observed. When the alkali ion is large, however, the electrostatic field is weaker and more diffuse, such that the rearrangement barrier may be difficult to traverse. This may allow sufficient time that thermalizing collisions then trap the ion in this excited conformation.

Support for the idea of an excited conformer comes from recent calculations performed by Hill and Feller, who examined this question in light of the present results.[47] They find a local minimum on the Rb^+(12c4) potential energy surface in which the Rb^+ ion is bound to the crown with S_4 symmetry (C_{2v} symmetry for the stucture overall). This minimum is located 55 kJ/mol above the ground state Rb^+(12c4) structure having C_4 symmetry. Thus, the excited conformer has a calculated BDE of ∼109 kJ/mol, in much better agreement with the experimental value of 95 ± 13 kJ/mol. The differences between experimental and theoretical BDEs for this conformer are now consistent with those of the DME complexes.

In the case of DXE complexes, the conformational problems are not as easily apparent; however, it is plausible that the metal ion interacts primarily with DXE in its more stable trans conformation (see Figure 2 of ref 21). This geometry allows a strong interaction with one of the oxygen atoms and limited access to the second. Rearrangement to the minimum-energy conformation in which the metal ion bisects the two oxygens can occur by rotation around the central C−C bond. This rotation has a barrier that is probably augmented by the presence of the metal ion because the positively charged hydrogens have to pass the positively charged metal ion in order to rotate into position. Again, we imagine that the more diffuse charge on the large ions makes it more difficult to overcome this barrier. If correct, this is apparently a problem for the second DXE ligand (where the charge is further delocalized by the presence of the first ligand) on Rb^+ and Cs^+ and for the first DXE ligand on Cs^+ but not Rb^+.

Trends in Bond Dissociation Energies. Several trends can be observed in the experimentally determined BDEs listed in Table 3. The BDEs for the $M^+(DME)_x$ complexes for both cations decrease monotonically as x increases. The average drop in the BDEs is 16 ± 4 and 11 ± 5 kJ/mol per additional DME ligand for Rb^+ and Cs^+, respectively. Likewise, the second DXE ligand is bound 49 ± 15 and 7 ± 9 kJ/mol more loosely than the first DXE for Rb^+ and Cs^+, respectively. These trends are in agreement with theory and conventional ideas of electrostatic ligation of gas-phase ions; viz., BDEs decrease with increasing ligation because of increasing ligand−ligand repulsion and increased charge solvation whereby the effective nuclear charge decreases.[48]

Not surprisingly, the bidentate ligand, DXE, is bound more strongly to Rb^+ than the monodentate DME ligand, but the tetradentate 12c4 ligand shows a BDE comparable to that for the DXE complex. This is consistent with Rb^+ interacting strongly with only two of the oxygens on the 12c4 ring. The Cs^+ complexes exhibit a different trend. The BDEs for Cs^+(DME) and Cs^+(DXE) are comparable, consistent with the idea that the DXE ligand uses only a single oxygen atom to bind to Cs^+. The BDE for Cs^+(12c4) is the largest of the complexes, but it is smaller than the sum of the BDEs for the first two DME ligands. This is also consistent with the idea that only two oxygens in the 12c4 ring are interacting with the Cs^+.

In our previous studies with the analogous Li^+, Na^+, and K^+ ether complexes[14−16] additional insight into the bonding and how it relates to the geometry of the complex was obtained by comparing the BDEs of like-alkali cation ether complexes that contained the same number of carbon and oxygen atoms. $M^+(DME)_2$ and M^+(DXE) form one such series, and $M^+(DME)_4$, $M^+(DXE)_2$, and M^+(12c4) comprise another. In the first series, the sum of the BDEs for $M^+(DME)_2$ exceeded the BDE for M^+(DXE) with ratios of 1:0.86 for M = Li,[14] 1:0.93 for M = Na,[15] and 1:0.86 for M = K.[16] The BDEs and BDE sums of the second series showed a similar pattern: $M^+(DME)_4 > M^+(DXE)_2 > M^+$(12c4). The ratios of the BDEs were 1:0.87:0.87, 1:0.93:0.86 and 1:0.86:0.80 for M = Li,[14] Na,[15] and K,[16] respectively. These patterns were rationalized by noting that the DME ligands are free to align their dipoles perfectly to interact with the M^+ ion core and to adjust their metal−ligand bond distances to optimum lengths. In contrast, the DXE and 12c4 ligands are unable to achieve perfect dipole alignment due to geometric constraints. The $M^+(DXE)_2$ complex is more stable than the M^+(12c4) because there are fewer constraints on dipole alignment and M^+−O distance for the DXE species than the 12c4 species. These results support similar conclusions drawn by Hay et al.,[49,50] who investigated structural requirements for strain-free metal ion complexation with aliphatic ethers using molecular mechanics and *ab initio* methods.

Table 4 lists the BDEs and BDE sums of the analogous Rb^+ and Cs^+ complexes. Examination of the Rb^+ and Cs^+ complexes' BDEs and BDE sums reveals that these complexes are quite different than the lighter alkali cations. For the series containing two oxygens, the BDEs and BDE sums again show $M^+(DME)_2 > M^+$(DXE) for both M = Rb and Cs. The ratios of these BDEs and BDE sums, 1:0.83 and 1:0.57 for M = Rb and Cs, respectively, indicate that the trend for Rb is comparable to the lighter alkali ions, but the BDE for Cs^+(DXE) relative to the sum for $Cs^+(DME)_2$ is considerably smaller than for the analogous complexes of the lighter alkali cations.[14−16] This

TABLE 4: Total Bond Dissociation Enthalpies at 298 K of $M^+(DME)_x$, $x = 2$ and 4, $M^+(DXE)_x$, $x = 1$ and 2, and $M^+(12c4)$ Where M = Rb and Cs in kJ/mol[a]

	2 oxygens		4 oxygens		
	$M^+(DME)_{1,2}$	$M^+(DXE)$	$M^+(DME)_{1-4}$	$M^+(DXE)_2$	$M^+(12c4)$
Rb	115(10)	95(9)	177(19)[b]	141(15)	95(13)
Cs	100(8)	57(5)	167(15)[b]	107(9)	86(9)

[a] Values taken from Table 3 with uncertainties given in parentheses. [b] The BDE for $M+(DME)_4$ is assumed to equal 0.87 of the BDE for $M^+(DME)_3$, the ratio found in the analogous K^+ complexes.[16]

weak bonding suggests that only one of the DXE oxygens interacts strongly to Cs^+, as described above. The BDEs and BDE sums of the second series where the ligands contain four oxygens follow the same qualitative trend as for the lighter alkalis,[14−16] but the ratios of the BDEs and BDE sums point to more anomalies. For this series, the ratios are 1:0.80:0.54 and 1:0.64:0.51 for the $M^+(DME)_4$:$M^+(DXE)_2$:$M^+(12c4)$ complexes for M = Rb and Cs, respectively. For both Rb and Cs, the BDE for $M^+(12c4)$ is about half the sum of the BDEs for $M^+(DME)_4$. As noted above, this suggests that these cations interact strongly with only two of the oxygens in 12c4. The sum of the $Cs^+(DXE)_2$ BDEs is much smaller than that for $Cs^+(DME)_4$ indicating that both the first and second DXE bonds are weaker than for the analogous complexes with lighter alkali ions. In the case of Rb^+, the ratio is somewhat smaller than for the lighter alkali cations because only the second bond to DXE is anomalously weak.

Comparison of Complexes with DME and H_2O. In our previous studies of Li^+, Na^+, and K^+ with one through four DMEs,[13,15,16] we examined how the BDEs of the ether complexes compare to the BDEs of the analogous water complexes. One might expect that the more polarizable DME ligands would yield greater cation−ligand BDEs than the less polarizable water ligand. Experimentally, we found that such relative BDEs are observed only for the Li^+ complexes,[13] while the analogous Na^+ and K^+ complexes with DME have BDEs that are either equal to or less than the Na^+ and K^+ complexes with H_2O.[15,16] This conclusion is understood by noting that the Na^+ and K^+ complexes have longer bond lengths that render the charge-induced dipole interaction (which scales as r^{-4} and dominates the M^+-DME interaction) relatively less important than the charge-dipole interaction (which scales as r^{-2} and dominates the M^+-H_2O interactions).

Figure 10 shows the experimentally determined BDEs of $M^+(DME)_x$, $x = 1-3$, and experimental BDEs for $M^+(H_2O)_x$, $x = 1-3$, determined by Dzidic and Kebarle[51] using high-pressure mass spectrometry,[50] for M = Rb and Cs. The BDEs for both sets of complexes decrease monotonically as x increases. The experimental BDEs for the $M^+(DME)_x$, $x = 1-3$, are lower than the $M^+(H_2O)_x$, $x = 1-3$, analogues by 8 ± 5 and 6 ± 4 kJ/mol for M = Rb and Cs, respectively. This difference is consistent with the relative BDEs of the DME and H_2O complexes for Na^+ and K^+, which showed differences of 4 ± 3 and 2 ± 1 kJ/mol, respectively.[15,16]

Conclusion

Kinetic energy dependent collision-induced dissociation in a guided ion beam mass spectrometer is used to determine the absolute bond dissociation energies of rubidium and cesium cation complexes with one to three dimethyl ether molecules, one and two 1,2-dimethoxyethane molecules, and the 12-crown-4 cyclic polyether. The experimental cross sections for the Rb^+ and Cs^+ complexes are comparable to the analogous smaller alkali metal cations complexes, which we have studied previously.[13−16] Analysis of the kinetic energy dependence of these cross sections, including considerations of the effects of multiple collisions, internal energies of the complexes, reactant translational energy distributions, and dissociation lifetimes, lead to the desired bond energies.

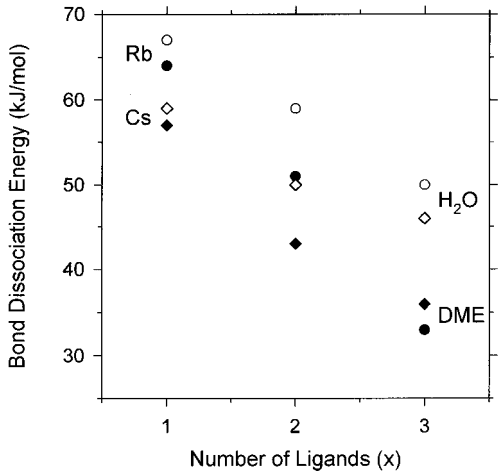

Figure 10. Bond dissociation energies at 298 K (in kJ/mol) of $(R2O)_{x-1}M^+-(OR2)$ where the R_2O ligand is dimethyl ether (R = CH_3, filled symbols, experimental results presented here, see Table 3 for uncertainties) and water (R = H, open symbols, experimental results taken from ref 50) plotted versus x. Circles and diamonds refer to M = Rb and Cs complexes, respectively.

The experimental bond dissociation energies obtained here are in good agreement with conventional ideas of electrostatic ligation of gas phase ions and recent results of *ab initio* calculations of Feller et al.[30,31] for the monodentate DME complexes (average discrepancy of 5 ± 6 kJ/mol). Poor agreement is observed for the multidentate DXE and 12c4 complexes (average discrepancy of 15 ± 5 kJ/mol per metal−oxygen interaction), except for $Rb^+(DXE)$. Several possible explanations for the discrepancies for the multidentate ligand complexes are considered. The most plausible is that the experimental results correspond to excited conformations of the $M^+(DXE)_x$ and $M^+(12c4)$ complexes, an idea supported by *ab initio* calculations.[47]

Acknowledgment. We thank E. D. Glendening, S. E. Hill, and D. Feller for sharing the results of their calculations prior to publication. Funding for this work was provided by the National Science Foundation under Grant CHE-9530412 (P.B.A.) and by the Division of Chemical Sciences, Office of Basic Energy Sciences, U.S. Department of Energy (M.B.M., D.R.). Pacific Northwest National Laboratory is operated for the U.S. Department of Energy by Battelle under Contract DE-AC06-76RLO 1830.

References and Notes

(1) See: *Principles of Molecular Recognition*; Buckingham, A. D., Roberts, S. M., Eds.; Blackie Academic and Professional: Glassglow, 1993.

(2) Izatt, R. M.; Rytting, J. H.; Nelson, D. P.; Haymore, B. L.; Christensen, J. J.; *Science* **1969**, *164*, 443. Izatt, R. M.; Bradshaw, J. S.; Nielsen, S. A.; Lamb, J. D.; Christensen, J. J.; Sen, D. *Chem. Rev.* **1985**, *85*, 271. Izatt, R. M.; Pawlak, K.; Bradshaw, J. S.; Bruening, R. L. *Chem Rev.* **1991**, *91*, 1721.

(3) See for example: Horwitz, E. P.; Dietz, M. L.; Fisher, D. E. *Solvent Extract. Ion Exchange* **1991**, *9*, 1. Moyer, B. A.; Delmau, L. H.; Case, G. N.; Bajo, S. Baes, C. F. *Sep. Sci. Technol*. **1995**, *30*, 1047.

(4) See for example: Grate, J. W.; Strebin, R.; Janata, J.; Egorov, O.; Ruzicka, J. *Anal. Chem.* **1996**, *68*, 333.

(5) Zhang, H.; Chu, I.-H.; Leming, S.; Dearden, D. V. *J. Am. Chem. Soc.* **1991**, *113*, 7415.

(6) Zhang, H.; Dearden, D. V. *J. Am. Chem. Soc.* **1992**, *114*, 2754.

(7) Chu, I.-H.; Zhang, H.; Dearden, D. V. *J. Am. Chem. Soc.* **1993**, *115*, 5736.
(8) Dearden, D. V.; Zhang, H.; Chu, I.-H.; Wong, P.; Chen, Q. *Pure Appl. Chem.* **1993**, *65*, 423.
(9) Maleknia, S.; Brodbelt, J. *J. Am. Chem. Soc.* **1992**, *114*, 4295.
(10) Brodbelt, J. S.; Liou, C.-C. *Pure Appl. Chem.* **1993**, *65*, 409.
(11) Katritzky, A. R.; Malholtra, N.; Ramanathan, R.; Kemerait, R. C., Jr.; Zimmerman, J. A.; Eyler, J. R. *Rapid Commun. Mass Spectrom.* **1992**, *114*, 2754.
(12) Cooks, R. G.; Kruger, T. L. *J. Am. Chem. Soc.* **1977**, *99*, 1279. McLucky, C. A.; Cameron, D.; Cooks, R. G. *J. Am. Chem. Soc.* **1981**, *103*, 1313.
(13) More, M. B.; Glendening, E. D.; Ray, D.; Feller, D.; Armentrout, P. B. *J. Phys. Chem.* **1996**, *100*, 1605.
(14) Ray, D.; Feller, D.; More, M. B.; Glendening, E. D.; Armentrout, P. B. *J. Phys. Chem.* **1996**, *100*, 16116.
(15) More, M. B.; Ray, D.; Armentrout, P. B. *J. Phys. Chem. A* **1997**, *101*, 831.
(16) More, M. B.; Ray, D.; Armentrout P. B. *J. Phys. Chem.*, in press.
(17) Loh, S. K.; Hales, D. A.; Lian, L.; Armentrout, P. B. *J. Chem. Phys.* **1989**, *90*, 5466.
(18) Ervin, K. M.; Armentrout, P. B. *J. Chem. Phys.* **1985**, *83*, 166.
(19) Schultz, R. H.; Armentrout, P. B. *Int. J. Mass Spectrom. Ion Processes* **1991**, *107*, 29.
(20) Aristov, N.; Armentrout, P. B. *J. Phys. Chem.* **1986**, *90*, 5135.
(21) Dalleska, N. F.; Honma, K., Sunderlin, L. S.; Armentrout, P. B. *J. Am. Chem. Soc.* **1994**, *116*, 3519.
(22) Chantry, P. J. *J. Chem. Phys.* **1971**, *55*, 2746.
(23) Schultz, R. H.; Armentrout, P. B. *J. Chem. Phys.* **1992**, *96*, 1046.
(24) Schultz, R. H.; Crellin, K. C.; Armentrout, P. B. *J. Am. Chem. Soc.* **1991**, *113*, 8590.
(25) Khan, F. A.; Clemmer, D. C.; Schultz, R. H.; Armentrout, P. B. *J. Phys. Chem.* **1993**, *97*, 7978.
(26) Fisher, E. R.; Kickel, B. L.; Armentrout, P. B. *J. Phys. Chem.* **1993**, *97*, 10204.
(27) Fisher, E. R.; Kickel, B. L.; Armentrout, P. B. *J. Chem. Phys.* **1992**, *96*, 4859.
(28) Beyer, T. S.; Swinehart, D. F. *Comm. Assoc. Comput. Machines* **1973**, *16*, 379. Stein, S. E.; Rabinovitch, B. S. *J. Chem. Phys.* **1973**, *58*, 2438. Stein, S. E.; Rabinovitch, B. S. *Chem. Phys. Lett.* **1977**, *49*, 183. Gilbert, R. G.; Smith, S. C. *Theory of Unimolecular and Recombination Reactions*, Blackwell Scientific Publications: Oxford, 1990.
(29) Shimanouchi, T. *Tables of Molecular Vibrational Frequencies: Consolidated Volume I*, NSRDS-NBS 39; U.S. Government Printing Office: Washington, DC, 1972.
(30) Hill, S. E.; Glendening, E. D.; Feller, D. *J. Phys. Chem.*, submitted for publication.
(31) Glendening, E. D.; Hill, S. E.; Feller, D. *J. Phys. Chem.*, submitted for publication.
(32) Chesvnavich, W. J.; Bowers, M. T. *J. Phys. Chem.* **1979**, *83*, 900.
(33) Armentrout, P. B. In *Advances in Gas Phase Ion Chemistry*; Adams, N. G., Babcock, L. M., Eds.; JAI: Greenwich, 1992; Vol. 1, pp 83−119.
(34) See for example: Sunderlin, L. S.; Armentrout, P. B. *Int. J. Mass Spectrom. Ion Processes* **1989**, *94*, 149.
(35) Dalleska, N. F.; Tjelta, B. L.; Armentrout, P. B. *J. Phys. Chem.* **1994**, *98*, 4191.
(36) Weber, M. E.; Elkind, J. L.; Armentrout, P. B. *J. Chem Phys.* **1986**, *84*, 1521.
(37) Dalleska, N. F.; Honma, K.; Armentrout, P. B. *J. Am. Chem. Soc.* **1993**, *115*, 12125. See Figure 1 of this reference.
(38) Boo, B. H.; Armentrout, P. B. *J. Am. Chem. Soc.* **1987**, *109*, 3459. Ervin, K. M.; Armentrout, P. B. *J. Chem. Phys.* **1987**, *86*, 2659. Elkind, J. L.; Armentrout, P. B. *J. Phys. Chem.* **1984**, *88*, 5454. Armentrout, P. B. In *Structure/Reactivity and Thermochemistry of Ions*; Ausloos, P.; Lias, S. G., Eds.; Reidel: Dordrecht, 1987; pp 97−164.
(39) Armentrout, P. B.; Simons, J. *J. Am. Chem. Soc.* **1992**, *114*, 8627.
(40) Hales, D. A.; Lian, L.; Armentrout, P. B. *Int. J. Mass Spectrom. Ion Processes* **1990**, *102*, 269.
(41) Rodgers, M. R.; Ervin, K. M.; Armentrout, P. B. *J. Chem. Phys.* **1997**, *106*, 4499.
(42) Rodgers, M. T.; Armentrout, P. B. *J. Phys. Chem. A* **1997**, *101*, 1238.
(43) Rodgers, M. T.; Armentrout, P. B. *J. Phys. Chem. A*, in press.
(44) Chase, M. W.; Davies, C. A.; Downey, J. R.; Frurip, D. J.; McDonald, R. A.; Syverud, A. N. *J. Phys. Chem. Ref. Data* **1985**, *14* (Suppl. No. 1).
(45) Hehre, W. J.; Ditchfield, R.; Pople, J. A. *J. Chem. Phys.* **1972**, *56*, 2257.
(46) Feller, D.; Apra, E.; Nichols, J. A.; Bernholdt, D. E. *J. Chem. Phys.* **1996**, *105*, 1940.
(47) Hill, S. E.; Feller, D. Unpublished results.
(48) See Natural Energy Decomposition Analysis of $Li^+(DME)_x$ clusters in ref 13.
(49) Hay, B. P.; Rustad, J. R. *J. Am. Chem. Soc.* **1994**, *116*, 6316.
(50) Hay, B. P.; Rustad, J. R.; Hostetler, C. J. *J. Am. Chem. Soc.* **1993**, *115*, 11158.
(51) Dzidic, I.; Kebarle, P. *J. Chem. Phys.* **1970**, *74*, 1466.